

# Stiffness Based Assessment of Masonry Arch Bridges

**Pardeep Kumar**

Associate Professor, Department of Civil Engineering, National Institute of Technology Hamirpur (HP) India,  
177005

Presenting author & Corresponding author: pardeepkumar.nit@gmail.com

## Abstract

There are numerous methods available on date for the structural assessment of masonry arch bridges. Each of these methods has been developed, at different times and places, having its own limitations of use and none of these is a commonly putative method. Among the problems of development of such an approach, the problem of selection of a suitable failure criterion for the prediction of the collapse load is critical. Particularly for arch bridges, involving moments, normal thrust and tangential thrust, the interaction of the axial force and the moments play a vital role in the choosing failure criteria. In view of this, different axial force and moment interactions are reviewed, along with the implementation of the same through a developed stiffness approach based on mechanism method for the prediction of load carrying capacity of the masonry arch bridges. The application of the method has been demonstrated on the bridges tested in field, and the load carrying capacity has been compared.

**Keywords:** Masonry, Stiffness, Arch Bridges, Mechanism, MEXE

## Notations

$[S_c]$	Complete structure stiffness matrix
$[\Delta_c]$	Complete joint displacement matrix
$[JL_c]$	Joint load matrix for complete structure
$[R_c]$	Complete support reaction matrix
$[K_i]$	Member stiffness matrix
$P_o$	Maximum concentric axial force
$M_o$	Maximum moment at an eccentricity of $d/4$
$\sigma_t$	Tensile strength of masonry

## Introduction

Masonry arch bridges have been a legacy of past, but are built hardly now-a-days. The newer materials with better structural properties have overshadowed the use of masonry and the art of masonry arches has been kerbed to the papers. In most of the countries where masonry arch bridges exist on railway and road network, the first choice of the bridge owners is to use MEXE (Military Engineering Experimental Establishment) [1] method for assessment of such bridges. This mechanism approach to arch collapse, originated from the first work of Pippard and Ashby [2] and Pippard [3]. The identification of location of a number of hinges at the arch intrados and extrados to transform it into a mechanism yielded the minimum load. The limit load is obtained through the application of the kinematic theorem [4] that takes the position of the hinges as the unknowns of the problem. This approach finds its latest results in the work by different authors [5]-[11]. The method was originally developed, based on the minimum strain energy principle and later used it during Second World War to develop tables of allowable weights for wheeled and tracked vehicles for military use [12]. The original MEXE method was then developed from these basic tables in form of readily usable

nomogram. The referred MEXE method is empirical and is a working stress method based on the elastic analysis but provides little information in regard to the considerations of the serviceability. All the subsequent methods are marginal improvement over the original one and have tried to overcome the shortcomings in the earlier methods. More so, with the increasing advent of computers, many computer based assessment methods have developed in recent years, which are in use in different parts of the world. To list, such methods include, CTAP developed by Bridle and Hughes, which is based on Castigliano's elastic strain energy method, MINIPONT developed by Department of Transport is computerized version of MEXE method, program ARCHIE developed by Harvey and Smith and program ARCH developed by Cascade Software Ltd [13]. The program ARCHIE and ARCH are based on the mechanism method of assessment. Heyman has described in detail the development and use of mechanism method of assessment [4].

Assessment of existing structures is always considered more tedious than the design of new structure. The confidence in new design can be well achieved through properly designing well understood part and relying on unquantified additional safety for the remainder part. Existing structures often rely on behaviours that the engineer prefers to keep as safety factor. How those actions are used in assessment is a matter for individual judgement and any guidance that obscures the reliance on alternative load paths is inherently dangerous because it reduces the scope of the engineer's judgement [14].

The assessed load carrying capacities of bridges using different methods also vary widely, due to variety of assumptions underlying the idealisation, load application, material properties, hinge formation criteria and mechanism etc. In the proposed formulation, the four obvious hinge positions are not selected, but, instead based upon the interaction of bending moment and axial force present at the section at different instants of loading, the successive formation of the hinges takes place until a mechanism is formed. The approach has been fully computerized through a program written in Fortran [15]. From the assessed capacity of a bridge, the procedure to determine the load rating is also laid down.

### **Experimental Investigation of Moment –Axial Force Interaction**

The control specimens were constructed in 1:4 cement sand mortar, having average cross-section 105 mm x 223 mm. Hand moulded class-A bricks of conventional size were used for the construction of prisms. The average height of the prisms was 681 mm, which was greater than the span of the test specimens. Three specimens were tested each at six different precompression levels. The arrangement was simply supported over the knife-edge supports to avoid any fixity. These were tested after curing of 28 days, under monotonically increasing two point load system at middle third points as shown in the Figure 1a. The test arrangement is shown in Figure 1b. The weight of the assembly was added to the load value. The experimental failure loads in masonry at different levels of precompression is given in Table 1.

The horizontal compressive force was applied along the centerline of the prism specimens. Three specimens each have been tested at different levels of the precompression corresponding to axial stress of 0%, 10%, 20%, 40%, 50%, and 60% of the crushing strength of the masonry from the uniaxial compression test on similar type of prism.

The bending tensile strength  $\sigma_t$  without any precompression can be found on equilibrating the internal and external moments, as given under.

$$\sigma_t = \frac{WL}{bd^2} \quad (1)$$

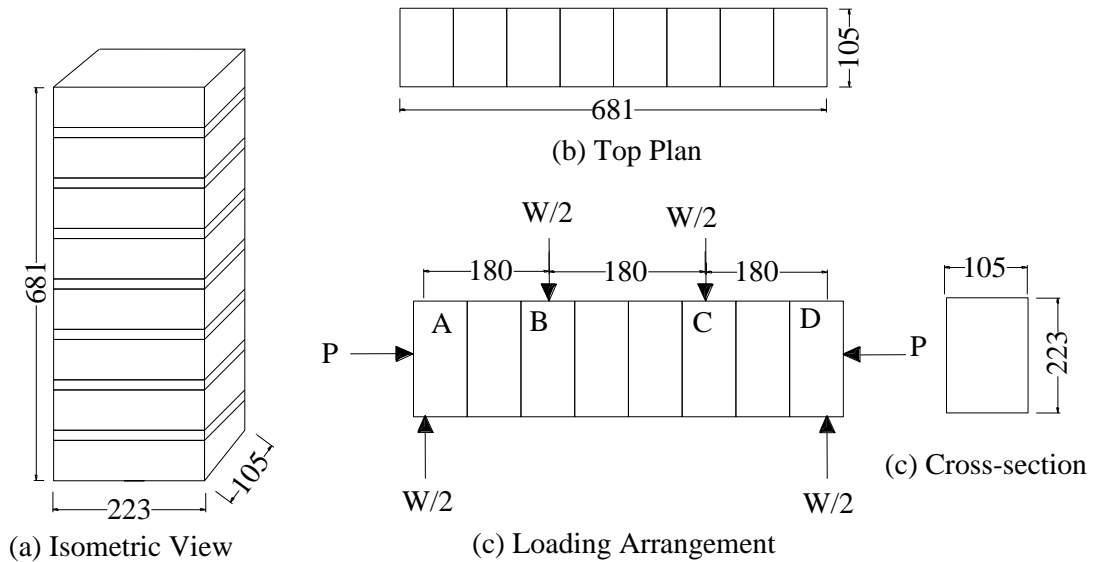


**Figure 1a Test specimen and loading details (Dimensions in mm)**

At 0% precompression, the bending tensile strength of the specimens tested has been determined as 0.29 N/mm<sup>2</sup>. The plot of non-dimensional parameters  $P/P_o$  versus  $M/M_o$  is drawn (Figure 2) for the experimental values. The axial loads are normalized with respect to  $P_o = \sigma_c b d$  and moments are normalized with respect to  $M_o = 0.125\sigma_c b d^2$ .

**Table 1. Experimental failure loads in masonry at different levels of precompression**

No. of specimens	Average size			Precompression		Exp. Failure Load, W (kN)
	Width, b (mm)	Depth, d (mm)	L (mm)	% of crushing strength	Load, P (kN)	
3	109.67	229.17	681	0	0.00	2.803
3	110.17	228.73	683	10	13.42	17.756
3	108.96	229.33	680	20	26.84	29.194
3	109.83	229.35	677	40	53.68	41.496
3	110.50	228.56	682	50	67.10	51.709
3	108.50	227.89	684	60	80.52	62.490

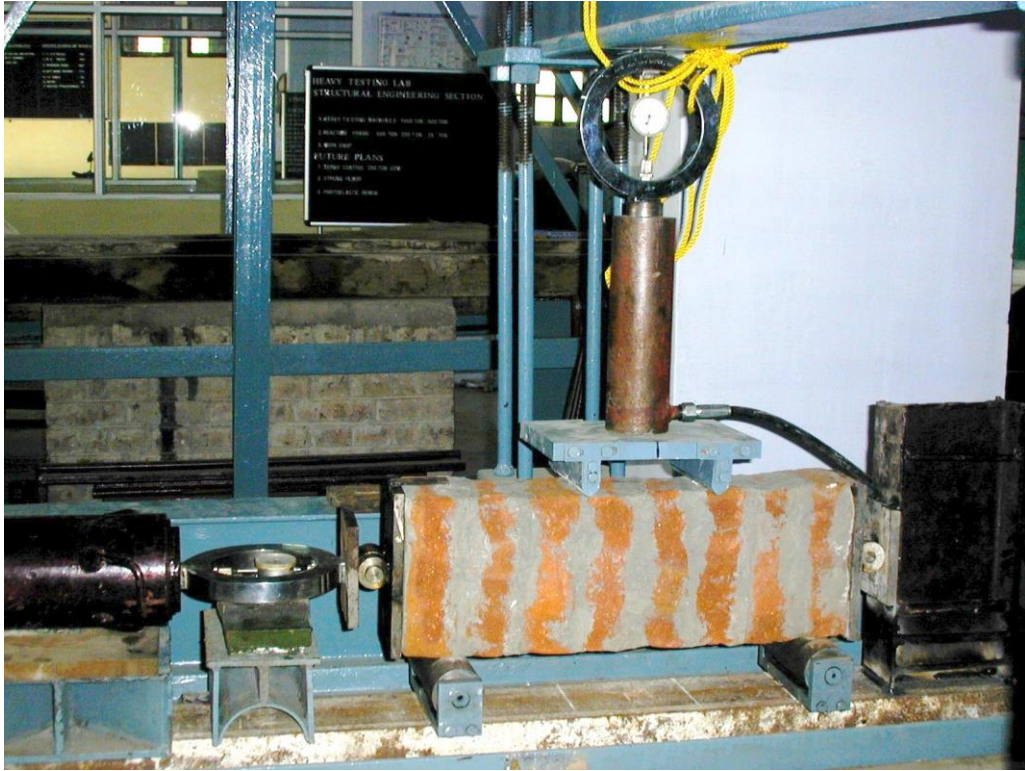


**Figure 1b Test arrangements for determination of flexural bond strength of masonry**

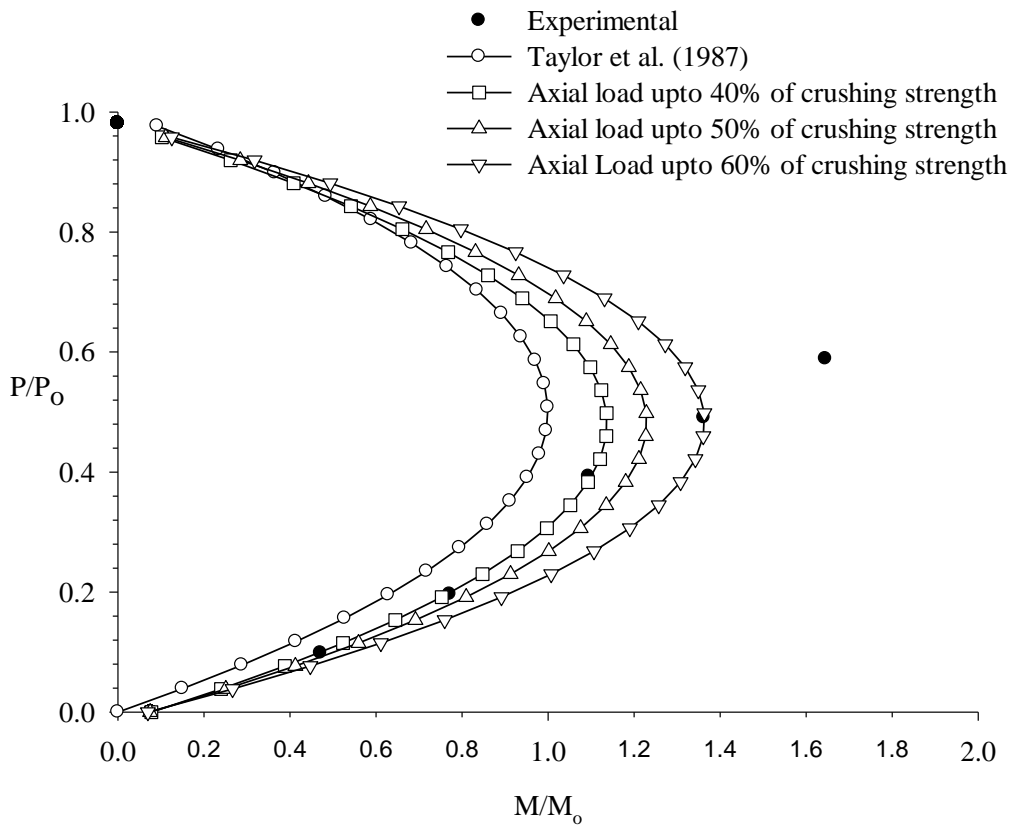


**Figure 2 Comparison of experimental axial force-moment interaction and limit state interaction developed by Taylor and Malinder [16]**

It has been observed during the testing that at higher precompression levels, with the increase in the transverse loads, the precompression automatically increased. Although, this has been taken care of by releasing the pressure in the load cell to maintain constant precompression. This may be one of the reasons that at precompression levels of 50% and 60% of crushing strength the transverse failure loads recorded are on the higher side, leading to  $M/M_o$  ratio greater than 1 as seen in Figure 2. The moment-axial force relationship has been extrapolated corresponding to all range of precompression levels and a parabolic equation is fitted to the normalized data as given under:

$$\frac{M}{M_o} = 0.0699 + 5.3476 \left( \frac{P}{P_o} \right) - 5.5224 \left( \frac{P}{P_o} \right)^2 \quad (2)$$

Keeping in view the problem encountered during the test program, the reliability of the point corresponding to precompression levels of 50% and 60% of crushing strength of masonry are low. Hence, discarding the points corresponding to these precompression levels modifies the best-fit equation and bring to the close proximity of that derived by Taylor and Mallinder [16]. Discarding the one point corresponding to precompression level of 60% of crushing strength would modify the equation as under:

$$\frac{M}{M_o} = 0.0751 + 4.7840 \left( \frac{P}{P_o} \right) - 4.9550 \left( \frac{P}{P_o} \right)^2 \quad (3)$$

Discarding two points corresponding to precompression levels of 50% and 60% of crushing strength modifies the equation as:

$$\frac{M}{M_o} = 0.0779 + 4.3994 \left( \frac{P}{P_o} \right) - 4.5662 \left( \frac{P}{P_o} \right)^2 \quad (4)$$

All these equations are plotted in Figure 2. Neglecting last two points provides an equation closely matching with the one available in the literature.

Taylor and Mallinder have reported the axial force/bending moment interaction for the limit state of rectangular masonry section. The strain distribution was assumed linear whereas a non-linear parabolic relation was assumed for the variation of stresses with strains. The moment-axial force interaction diagram represented by Eqns. 2, 3, and 4 has been compared in Figure 2 with that of analytically developed interaction (Eqn. 5) by Taylor and Mallinder [16].

$$\frac{M}{M_o} = 4 \left( \frac{P}{P_o} \right) - 4 \left( \frac{P}{P_o} \right)^2 \quad (5)$$

The proposed interaction equations take into account the masonry tensile strength, indicated by the presence of constant term in the equations. Despite the lack of the sophisticated equipment used in the present investigation, a reasonable correlation has been obtained.

### The Basis of Proposed Method

Although the behaviour of the arches is fundamentally non-linear due to the axial force-moment interaction, the proposed method utilizes linear elastic theory. The linear elastic analysis under the action of unit live load is carried out and the load factors are computed by steering the analysis moments and axial forces to satisfy the axial force-moment interaction to incorporate plastic hinge at appropriate locations, until the formation of a collapse mechanism.

The moment-axial force interaction is the most important parameter to determine the load carrying capacity of the masonry arch bridges. Wherever the combination of moment and axial force developed in the section lies on this surface, a hinge shall be assumed to form at that section and the hinge will continue to rotate when further load is applied till the arch is converted to a mechanism.

Considering the unit width of the arch ring, it can be divided into a sufficient number of segments along the barrel centerline. Each segment can be assumed to be a straight line joining the two nodes. These segments can be represented by a beam element having appropriate material and sectional properties. The end nodes are fixed at the springing line to provide restraint against any horizontal, vertical, or rotational movement. The arch is analysed first under the dead loads imposed due to self-weight of the arch ring and the load of the overlaying fill. The weight of the fill is calculated over each segment and is applied as equivalent nodal loads at its two nodes. The arch is then analysed under a unit live load applied at quarter point. The obtained values of bending moment and axial force due to dead and live load so obtained are modified to satisfy the limit state envelope at every node. A step-by-step linear analysis is performed to locate the four hinge locations and the corresponding total load on the bridge is the failure load. The details of the method are reported elsewhere [15].

### **The Stiffness Method**

The proposed formulation is based on stiffness approach, where a set of simultaneous equations in form of matrices are developed and solved. The representative set of equation can be expressed as

$$[S_c][\Delta_c] = [JL_c] + [R_c] \quad (6)$$

Defining  $[S_c]$  as the complete structure stiffness matrix,  $[\Delta_c]$  as the complete joint displacement matrix,  $[JL_c]$  as the complete joint load matrix, and  $[R_c]$  as complete support reaction matrix. In the development of the several matrices of Eqn. 6 all components of joint displacement, joint load and support reaction, which form the elements of respective matrices, must be described with respect to a same system of axes, i.e. the reference axes for the entire structure. The formulation of this method is given in many standard texts [17][18].

Each segment is modelled as a beam element that has either constant or variable moment of inertia over its length positioned in the local axis  $X_m$ - $Y_m$ , with origin at j-end of the member and  $X_m$  axis directed towards k-end of the member. If the beam element is subjected to general displacements  $\theta_p$ ,  $\theta_q$ ,  $\delta_r$ ,  $\delta_s$ ,  $\delta_t$  and  $\delta_u$  of its ends, the resulting end actions can be determined as shown in Figure 3. Hence, the force - displacement relationship in local system, for a prismatic member can be expressed as given by Eqn. 7.

## The Beam Element

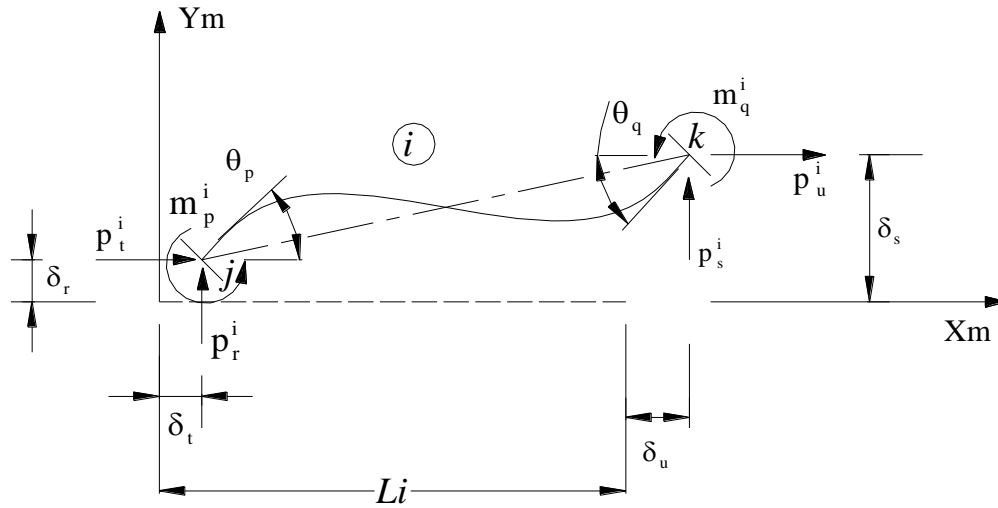


Figure 3 General displacement of a typical beam element with restrained ends.

$$\begin{Bmatrix} m_p^i \\ m_q^i \\ p_r^i \\ p_s^i \\ p_t^i \\ p_u^i \end{Bmatrix} = \begin{bmatrix} \frac{4EI}{L} & \frac{2EI}{L} & \frac{6EI}{L^2} & \frac{-6EI}{L^2} & 0 & 0 \\ \frac{2EI}{L} & \frac{4EI}{L} & \frac{6EI}{L^2} & \frac{-6EI}{L^2} & 0 & 0 \\ \frac{6EI}{L^2} & \frac{6EI}{L^2} & \frac{12EI}{L^3} & \frac{-12EI}{L^3} & 0 & 0 \\ \frac{-6EI}{L^2} & \frac{-6EI}{L^2} & \frac{-12EI}{L^3} & \frac{12EI}{L^3} & 0 & 0 \\ \frac{L^2}{L^2} & \frac{L^2}{L^2} & \frac{L^3}{L^3} & \frac{L^3}{L^3} & 0 & 0 \\ 0 & 0 & 0 & 0 & \frac{AE}{L} & \frac{-AE}{L} \\ 0 & 0 & 0 & 0 & \frac{-AE}{L} & \frac{AE}{L} \end{bmatrix} \begin{Bmatrix} \theta_p \\ \theta_q \\ \delta_r \\ \delta_s \\ \delta_t \\ \delta_u \end{Bmatrix} \quad (7)$$

$$\{p_i\} = [K_i]\{\delta_i\} \quad (8)$$

where the matrix  $\{\delta_i\}$  represent the components of end displacements of member i, the matrix  $\{p_i\}$  represents the components of end actions required to maintain equilibrium of member i when subjected to general end displacements and the matrix  $[K_i]$  represent the components of member end actions resultant from independent application of unit values of the possible end displacements. This is also referred to as member stiffness matrix.

### Transformation Matrix: Beam Element

For general end displacements of the restrained member, the components of end actions have been defined with respect to the local axis. The components of end actions in local axes can be transformed in terms of the components of end actions with in the frame of the global axes as

$$\{p_i\} = [T_i]\{\bar{p}_i\} \quad (9)$$

where the matrix  $\{p_i\}$  represents the components of end actions for member i in local system; the matrix  $\{\bar{p}_i\}$  represents the components of end action for member i in the frame of global axes and  $[T_i]$  is the transformation matrix as given below.

$$[T_i] = \begin{bmatrix} 1 & 0 & 0 & 0 & 0 & 0 \\ 0 & 1 & 0 & 0 & 0 & 0 \\ 0 & 0 & C_x & 0 & -C_y & 0 \\ 0 & 0 & 0 & C_x & 0 & -C_y \\ 0 & 0 & C_y & 0 & C_x & 0 \\ 0 & 0 & 0 & C_y & 0 & C_x \end{bmatrix} \quad (10)$$

where  $C_x$  and  $C_y$  are direction cosines.

On the similar basis the relation between the components of end displacements of member i with respect to local axis  $X_m$ - $Y_m$  and the reference axes  $X$ - $Y$  can be established as

$$\{\delta_i\} = [T_i] \{\bar{\delta}_i\} \quad (11)$$

where matrix  $\{\delta_i\}$  represents the components of member end displacements in the system of local axes and the matrix  $\{\bar{\delta}_i\}$  represents the components of member end displacements in a system of global axes.

Thus Eqn. 13 gives member stiffness matrix with respect to global axes.

$$\{\bar{p}_i\} = [T_i]^T [K_i] [T_i] \{\bar{\delta}_i\} \quad (12)$$

$$[\bar{K}_i] = [T_i]^T [K_i] [T_i] \quad (13)$$

is defined as the transformed member stiffness matrix expressed with respect to the arbitrary system of global axes  $X$ - $Y$ . The Eqn. 11 describes the relationship between the components of the end displacements and the end actions of member i in the frame of global axes. Once the system of equilibrium equations are generated in the global axes, the independent components of the unrestrained joint displacements are evaluated by substituting the boundary conditions and solving the set of residual equations expressed as

$$[S_{uu}] [\Delta_u] = [JL_u] \quad (14)$$

and the components of the support reactions are determined by solving that set of equations expressed as

$$[S_{ru}] [\Delta_u] - [JL_r] = [R_r] \quad (15)$$

## Assumptions of Method

The method is based on the following assumptions:

- At the point of hinge the axial force and shear force resisting capacity is not impaired and it continues to resist the axial force and shear force.
- The effect of the shear forces on moment-axial force interaction envelope has been ignored.
- The point where a hinge is formed will continue to rotate.

## Comparison of Proposed Analysis to Field Results

In order to validate the proposed model for indigenous constructions, the two sets of arches were constructed and tested in the laboratory. The description of these arches can be found elsewhere [19]. The material properties and other input data used in the analysis are tabulated in Table 2. The obtained results with different axial force moment interaction have been compared with the experimental results in Table 3.

From the comparison of the results, it can be observed that inclusion of tensile strength of the masonry considerably improves the results. The loads predicted by using Eqn. 2 are in excess of test maximum loads. The estimated load carrying capacity is 40.94% in excess for first set of arches and 38.41% in excess for second set of arches in comparison to the experimental loads. The use of Eqn. 4 can reliably simulate the test results using the material properties given in Table 2. These properties have achieved through the experimental investigations on the indigenous masonry in the laboratory. The estimated load carrying capacity is only 11.96 % in excess for first set of arches and 5.52 % in excess for second set of arches in comparison to the experimental loads. On the other hand, using Eqn. 5 derived by Taylor and Mallinder [16], the estimated load carrying capacity is too low in comparison to the test results for both the sets of test arches. In view of this the equation derived from the experimental investigations after neglecting the points with unreliable data is proposed to be used for correctly predicting the load carrying capacity of a masonry arch bridge in fairly good condition with indigenous constructions.

**Table 2. Material properties used in the analysis**

Material	Property	Value	Units
Brick Masonry	Modulus of Elasticity	3723	N/mm <sup>2</sup>
	Compressive Strength	5.84	N/mm <sup>2</sup>
	Tensile Strength	0.29	N/mm <sup>2</sup>

**Table 3. Comparisons of failure loads (kN)**

Bridge	Test Maximum Load (kN)	Load Predicted from Proposed Method (kN)		
		Using Eqn. 2	Using Eqn. 4	Using Eqn. 5
Arches AV1 & AV2	55.10 *	77.66	61.69	31.36
Arches AF1 & AF2	74.25 *	103.07	78.35	55.55

\* The values are average for the two similar models.

Because of the difference in the method of analysis (Step-by-step linear) and the actual behaviour (non-linear) of the structures it is difficult to get the actual response of the structures from the proposed analysis. The load-deflection response achieved from the structures has been compared with the experimental behaviour of both the set of the arches. The comparison of the load deflection under the load point for test arches is shown in Figures 4 and 5 respectively. The predicted average deflections for test arches AV1 and AV2 are only 8.7 % of the experimentally observed value and 31.2 % for arches AF1 and AF2. It can be inferred from the comparison that the method can predict the load carrying capacity but not the deflections.

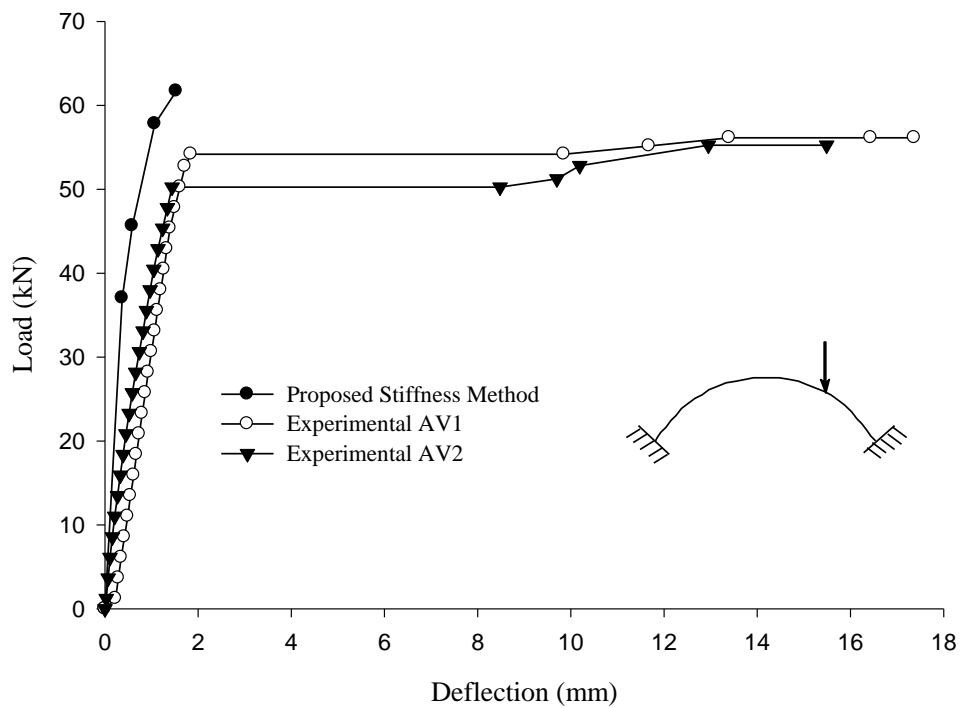


**Figure 5 Comparison of predicted and experimental load-deflection behaviour of the arches AV1 and AV2**

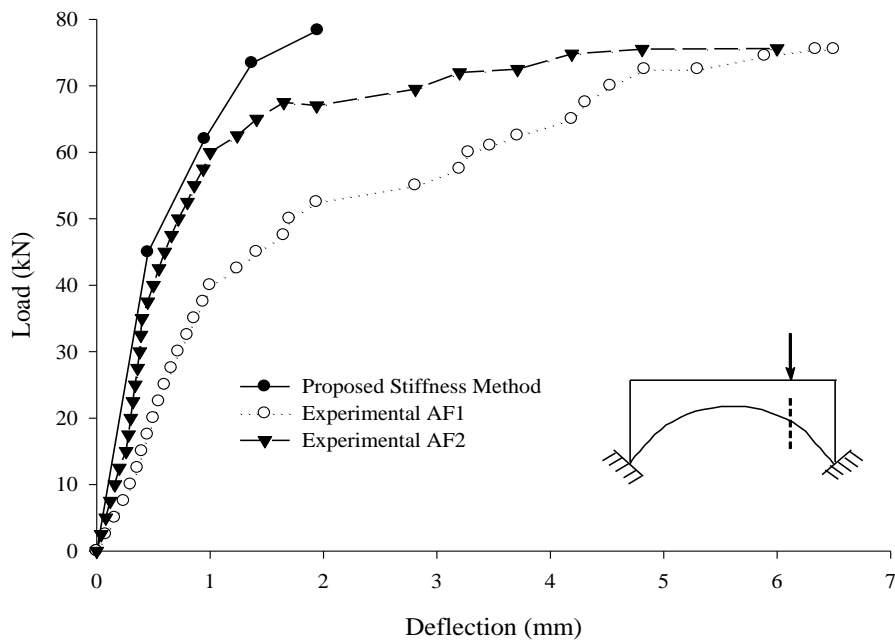


**Figure 6 Comparison of predicted and experimental load-deflection behaviour of the arches AF1 and AF2**

### Conclusions

The axial force-moment interaction can be effectively used for the prediction of load carrying capacity of the masonry arch bridges. In the proposed method the experimentally determined axial force-moment interaction has been verified and implemented successfully to predict the

collapse load. The method can predict the load carrying capacity within an acceptable range of variation. For first set of test arches the predicted values differ by 11.56 % and by 5.52 % for second set of test arches. The predicted values are on higher side, which may be attributed to the use of material properties determined from the control specimens.

The proposed interaction, accounts for some minimum tensile strength of the masonry. The proposed method can predict the collapse load on the basis of formation of adequate number of hinges leading to conversion to a mechanism.

The frame analysis program automated for the formation of the hinges and further leading to failure on formation of the mechanism provides a sufficiently quick and simple method for determination of the load carrying capacity of the masonry arches assuming a unit width of the arch ring.

### **Acknowledgement**

The help rendered by Professor N. M. Bhandari, Professor at IIT Jodhpur, is duly acknowledged for the development of the frame analysis program automated for the formation of the hinges and further leading to failure on formation of the mechanism.

### **References**

- [1] Department of Transport, (2001) Assessment of Masonry Arch Bridges by Modified MEXE Method”, Vol. 3, Section 4, Part 4 BA 16/97, Amendment No. 2.
- [2] A J S Pippard and R J Ashby, An Experimental Study of The Voussoir Arch. (Includes Photographs, Plates And Appendix), Volume 10 Issue 3, January 1939, pp. 383-404.
- [3] Pippard, A. J. S., “The Approximate Estimation of Safe Loads on Masonry Arch Bridges”, Civil Engineer in war, Vol. 1, 365, Institution of Civil Engineers, London, 1948.
- [4] Heyman, J., (1982) The Masonry Arch, Ellis Horwood, Chichester.
- [5] Crisfield, M.A., Packham, A.J., (1988). A mechanism program for computing the strength of masonry arch bridges, Transport and Road Research Laboratory, Dept. of Transport, Research Report 124.
- [6] Harvey, W.E.J., (1988). Application of the mechanism analysis to masonry arches, The Structural Engineer, 66, 77-84.
- [7] Blasi, C., Foraboschi, P., (1994). Analytical approach to collapse mechanisms of circular masonry arches, J. Struct. Engrg., ASCE, 120, 2288-2309.
- [8] Falconer, R.E., (1994). Assessment of multi-span arch bridges, Proc. 3rd Int. Conf. on Inspection, Appraisal, Repair and Maintenance of Buildings and Structures, Bangkok, 79-88.
- [9] Gilbert, M. and Melbourne, C., (1994). Rigid-block analysis of masonry structures, The Str. Eng., 72, 356- 361.
- [10] Hughes, T.G., (1995). Analysis and assessment of twin-span masonry arch bridges, Proc. Instn. Civ. Engrs., 110, 373-382.
- [11] Como, M., (1998). Minimum and maximum thrusts states in Statics of ancient masonry bridges, Proc. II Int. Arch Bridge Conf., A. Sinopoli ed., Balkema, Rotterdam, 321-330.
- [12] Pippard A. J. S. and Chitty L. A., (1951) Study of the voussoir arch, National Building Studies Research Paper No. 11, HMSO London.
- [13] Ng, K. H., Fairfield, C. A., (1999) Finite Element Analysis of Masonry Arch Bridges, Proc. Instn. Civ. Engrs. Structs. & Bldgs, Vol. 134, pp. 119-127.
- [14] Harvey, Bill, Kumar, Pardeep and Bhandari, N. M., (2007) Mechanism Based Assessment of Masonry Arch Bridges SEI Discussion, Structural Engineering International, Vol. 17, Number 1, pp. 97-99.
- [15] Kumar, Pardeep and Bhandari, N. M., (2006) Mechanism Based Assessment of Masonry Arch Bridges IABSE quarterly publication Structural Engineering International, Vol. 16, Number 3, pp. 226-234.
- [16] Taylor, N. and Mallinder, P., (1987) On Limit State Properties of Masonry, Proceedings Institution of Civil Engineers, Part 2, Vol. 83, pp. 33-41.
- [17] Weaver W. and Gere, J. M., (1986) Matrix Analysis of Framed structures, Second Edition, CBS Publishers and Distributors, Delhi, India.
- [18] Beaufait, F. W. et al., (1970) Computer Methods of Structural Analysis, Prentice Hall.
- [19] Kumar, Pardeep, (2005) Load Rating and Assessment of Masonry Arch Bridges, Ph.D. Thesis, Indian Institute of Technology, Roorkee.